Variations of Mediterranean–Atlantic exchange across the late Pliocene climate transition

Ángela García-Gallardo[1], Patrick Grunert[1,2], Werner E. Piller[1]

[1]Institute of Earth Sciences, University of Graz, NAWI Graz Geocenter, Heinrichstrasse 26, 8010 Graz, Austria.

[2]Institute of Geology and Mineralogy, University of Cologne, Zülpicher Strasse 49a, 50674 Cologne.

Correspondence to: Ángela García-Gallardo (angela.garcia-gallardo@uni-graz.at)

Abstract. Mediterranean-Atlantic exchange through the Strait of Gibraltar plays a significant role in the global ocean-climate dynamics in two ways. On one side, the injection of the saline and warm Mediterranean Outflow Water (MOW) contributes to North Atlantic deep-water formation. In return, the Atlantic inflow is considered a sink of less saline water for the North Atlantic Ocean. However, while the history of MOW is the focus of numerous studies, the Pliocene Atlantic inflow has received little attention so far. The present study provides an assessment of the Mediterranean–Atlantic exchange with focus on the Atlantic inflow strength and its response to regional and global climate from 3.33 to 2.60 Myrs. This time interval comprises the mid-Pliocene warm period (MPWP, 3.29–2.97 Myr) and the onset of the Northern Hemisphere Glaciation (NHG). For this purpose, gradients in surface $\delta^{18}O$ records of the planktonic foraminifer *Globigerinoides ruber* between the Integrated Ocean Drilling Program (IODP) Hole U1389E (Gulf of Cadiz) and Ocean Drilling Program (ODP) Hole 978A (Alboran Sea) have been evaluated. Interglacial stages and warm glacials of the MPWP revealed steep and reversed (relative to the present) W-E $\delta^{18}O$ gradients suggesting a weakening of Mediterranean–Atlantic exchange likely caused by high levels of relative humidity in the Mediterranean region. In contrast, periods of stronger inflow are indicated by flat $\delta^{18}O$ gradients due to more intense arid conditions during the severe glacial Marine Isotope Stage (MIS) M2 and the initiation of the NHG (MIS G22, G14, G6–104). Intensified Mediterranean–Atlantic exchange in cold periods is linked to the occurrence of ice-rafted debris (IRD) at low latitudes and weakening of the Atlantic Meridional Overturning Circulation (AMOC). Our results thus suggest the development of a negative feedback between AMOC and exchange rates at the Strait of Gibraltar in the latest Pliocene as it has been proposed for the late Quaternary.

Keywords. Atlantic inflow; Mediterranean Outflow Water; *Globigerinoides ruber*; oxygen isotopes; Mid-Pliocene Warm Period; Northern Hemisphere Glaciation.

1 Introduction

Mediterranean–Atlantic water mass exchange through the Strait of Gibraltar is driven by a two directional current system in which the westward outflow of warm and saline Mediterranean Outflow Water (MOW) at the bottom, driven by excess evaporation in the Mediterranean, is compensated by the inflow of colder and less saline North Atlantic Central Water (NACW) at the surface (Bormans et al., 1986; Ochoa and Bray, 1991; Vargas-Yáñez et al., 2002). This exchange plays an important role for regional and global climate in two respects. First, the injection of warm and salty MOW into the North Atlantic contributes to deep water formation at high latitudes, and thus to the dynamics of the ocean–climate system (Bryden and Kinder, 1991; Ivanovic et al., 2014; Reid, 1979; Rogerson et al., 2012; Voelker et al., 2006). Second, the eastward Atlantic inflow has been considered a freshwater sink for the North Atlantic since less saline North Atlantic Central Water is replaced with saltier MOW (Rogerson et al., 2010). Periods of stronger MOW correspond to weak phases of Atlantic Meridional Overturning Circulation (AMOC) resulting in a negative feedback between exchange and AMOC recognized during Heinrich Stadials in the late Quaternary (Rogerson et al., 2010, 2012).

Previous research has focused strongly on MOW variability since the Pliocene (e.g. Bryden and Stommel, 1982; Hernández-Molina et al., 2014; Iorga and Lozier, 1999; Kaboth et al., 2016; Voelker et al., 2006) but has neglected the Atlantic surface water component (Rogerson et al., 2010). Furthermore, there are a number of studies on Mediterranean–Atlantic exchange during the early-mid Pliocene and early Pleistocene (e.g., Bahr et al., 2015; García-Gallardo et al., 2017; Grunert et al., 2017; Hernández-Molina et al., 2014; Kaboth et al., 2017; Khélifi et al. 2009, 2014; Van der Schee et al., 2016; Voelker et al., 2015) leaving a gap in our knowledge about the late Pliocene climate transition comprising the mid-Pliocene warm period (MPWP) and the initiation of the Northern Hemisphere Glaciation (NHG).

The MPWP (3.29–2.97 Myr) has been identified by the United States Geological Survey's PRISM (Pliocene Research, Interpretation and Synoptic Mapping; Dowsett et al., 2010) group as a potential analogue for the future of global climate due to remarkable similarities with model predictions (Dowsett et al., 2012;

Robinson et al., 2008). These include increased levels of greenhouse gases up to 350–450 ppmv, global temperatures increased by 1–5 °C relative to today, and increased annual precipitation and elevated sea level as projected from data and models (Budyko et al., 1985; Fauquette et al., 1998; Haywood and Valdes, 2004; Lunt et al., 2012; Pagani et al., 2010; Raymo et al., 1996; Seki et al., 2010). At ~3.3 Ma, a severe ice sheet expansion initiated glacial Marine Isotopic Stage (MIS) M2, a precursor for the initiation of NHG at 2.95 Ma (Bartoli et al., 2006). The strong glacial at MIS M2 have been considered the first severe cold period before the NHG in which long-term intensification of Mediterranean–Atlantic exchange occurred (Khélifi et al., 2014; Sarnthein et al., 2017).

The present study aims for the reconstruction of variations in Mediterranean–Atlantic exchange with strong focus on the Atlantic inflow throughout the MPWP and the onset of the NHG. The Integrated Ocean Drilling Program (IODP) Hole U1389E has been used as the reference location for the Gulf of Cadiz and Ocean Drilling Program (ODP) Hole 978A for the Alboran Sea (Fig. 1). Planktonic $\delta^{18}O$ records obtained from both sites were used for the reconstruction of isotopic gradients as indicators of Atlantic inflow strength across the late Pliocene climate transition.

2 Regional setting

2.1 Alboran Sea – ODP Hole 978A

ODP Hole 978A is located in the Alboran Sea north of the Al-Mansour Seamount (36°13'N, 02°03'W; Fig. 1) at 1930 m water depth (Comas et al., 1996). Circulation in the Alboran Sea is driven by three water mass layers. At the surface (0 – ~200 m), inflowing Atlantic water enters the Mediterranean basin (Millot, 1999). On its way, it mixes with upwelled MOW within the Strait of Gibraltar (Folkard et al., 1997) and with surface waters of the Alboran Sea, creating the Modified Atlantic Water with temperatures of 15–16 °C and salinity of 36.5 (Millot, 1999), which follows two anticyclonic gyres, the Western Alboran Gyre (WAG) and the Eastern Alboran Gyre (EAG; Fig. 1) (Gascard and Richez, 1985; Vargas-Yáñez et al., 2002). The northern Alboran Sea is affected by upwelling along the Spanish coast providing nutrients and enhanced primary productivity (Minas et al., 1991; Peeters et al., 2002; Sarhan et al., 2000). The bottom layer is represented by the Western Mediterranean Deep water (WMDW; water temperature ~ 13 °C, salinity ~ 38.5) below 1000 m, formed due to overturning in the Gulf of Lions (Bryden et al., 1994;

Hernández-Molina et al., 2006; Millot, 1999; Rhein, 1995). The intermediate layer found between ~ 200 and 1000 m is composed of the salty (up to 39.1) and warm (14.7 to 17 °C) Levantine Intermediate water (LIW) which originates from overturning in the Eastern Mediterranean (Fig. 1; Millot, 2013; Wüst, 1961). Finally, WMDW, together with LIW, exit the Mediterranean basin through the Strait of Gibraltar and form MOW in the Gulf of Cadiz (Bryden et al., 1994).

2.2 Gulf of Cadiz – IODP Hole U1389E

IODP Hole U1389E is located in the northern Gulf of Cadiz (36°25.515'N, 07°16.683'W; Fig. 1) at 644 m water depth under direct influence of MOW (Fig. 1). It constitutes a key site for the recovery of an upper Pliocene contourite succession (Stow et al., 2013). Once LIW and WMDW exit the Strait of Gibraltar and form MOW, this water mass splits into two plumes due to the complex morphology of the continental slope in the Gulf of Cadiz. The upper plume flows between 500 and 800 m while the lower plume flows between 800 and 1400 m (Ambar and Howe, 1979; Borenäs et al., 2002; García et al., 2009; Llave et al., 2007; Madelain, 1970; Marchès et al., 2007; Serra et al., 2005; Zenk, 1975). Surface circulation in the Gulf of Cadiz is governed by the Gulf of Cadiz slope current (Fig. 1), flowing eastward along the western Iberian margin and the offshore inflow which meet at the Strait of Gibraltar and enter the Mediterranean basin (Peliz et al., 2009).

3 Material and methods

3.1 Sample material and data collection

This study relies on published and newly acquired stable oxygen isotope ($\delta^{18}O$) records of the planktonic foraminifer *Globigerinoides ruber* from upper Pliocene (3.33–2.60 Myrs) sediments at ODP Hole 978A (Alboran Sea), IODP Hole U1389E (Gulf of Cadiz) and the Rossello section in Sicily (Fig. 1). Sediment cores from ODP 978A were recovered during ODP Leg 161 (Comas et al., 1996). Khélifi et al. (2014) have established a $\delta^{18}O$ record from *Gs. ruber* for this site which ranges from 3.60 to 2.70 Myrs (cores 26R–20R, 438.38–371.00 mbsf). For the purpose of our study, this record was extended to 2.60 Ma through analyses of new samples collected every 50 cm from core sections 19R-5 through 16R-4 at the Bremen Core Repository.

Sediment cores from IODP Hole U1389E were obtained during IODP Expedition 339 (Stow et al., 2013). A $\delta^{18}O$ record of *Gs. ruber* ranging from 3.70 to 2.60 Myrs (cores 70R–41R, 982.78–703.62 mbsf) has been established by Grunert et al. (2017) and adopted for this study.

The stacked $\delta^{18}O$ record of Lourens et al. (1992, 1996) from the Rossello outcrops in Sicily has been adopted for stratigraphic calibration of the new $\delta^{18}O$ record at ODP Hole 978A.

3.2 Stable isotope analysis

Details on laboratory protocols and isotopic analyses performed by Grunert et al. (2017), Khélifi et al. (2014) and Lourens et al. (1996) can be found in the respective publications. For the continuation of the ODP 978A record, 46 samples from core-sections 19R-5 to 17R-1 were analyzed every 50 cm. Sediment samples were dried, weighed, washed through sieves 250 and 63 µm and dried. Whenever possible, 10 to 20 well-preserved specimens of *Gs. ruber* > 250 µm were picked for isotopic analysis. Shells were crushed, cleaned in a H_2O_{dest} : Methanol (2:1) mixture and ultrasonic-bathed for 1 minute. Clean shells were reacted with 100% phosphoric acid at 70 °C using a Gasbench II connected to a ThermoFisher Delta V Plus mass spectrometer at GeoZentrum Nordbayern (Erlangen). All values are reported in per mil relative to Vienna Pee Dee belemnite (VPDB). Reproducibility (±1σ) and accuracy were monitored by replicate analysis of laboratory standards calibrated by assigning $\delta^{13}C$ values of +1.95‰ to NBS19 and -46.6‰ to LSVEC and $\delta^{18}O$ values of -2.20‰ to NBS19 and -23.2‰ to NBS18.

3.3 Age model

Age constraints for ODP Hole 978A are established from 3.6 to 2.8 Myrs by Khélifi et al. (2014) and those for IODP Hole U1389E are reported in Grunert et al. (2017). The latter study establishes the correlation of the $\delta^{18}O$ record of IODP U1389E to ODP 978A from Khélifi et al. (2014). However, in the upper part (< 2.75 Ma), IODP U1389E is correlated to the Rossello section because ODP 978A record ends there. To ensure comparability, the newer $\delta^{18}O$ record obtained in this study for the upper ODP 978A has been visually correlated to the Rossello section. Biostratigraphic events have been adopted from Comas et al. (1996) for ODP 978A and from Lourens et al. (1996) for the Rosello section to warrantee a precise correlation (Fig. 2-a; Table 1). The last occurrence (LO) of the calcareous nannofossil *Discoaster tamalis* (2.78 Ma) delimits ODP 978 at the bottom of the studied interval (Fig. 2) while the top is demarcated by the LO of *D. pentaradiatus* (2.52 Ma; Comas et al., 1996). In the Rossello section, the bottom of the studied interval includes the first occurrence (FO) of the planktonic foraminifer *Neogloboquadrina*

atlantica (sin) (2.72 Ma) while the top is delimited by the LO of the calcareous nannofossils *D. pentaradiatus* and *D. surculus* (2.51 and 2.55 Ma, respectively; Lourens et al., 1996). Marine Isotopic Stages (MIS) have been identified by visual correlation with the Rossello Section (Lourens et al., 1996; Figs. 3, 4-a), which was in turn correlated to the LR04 benthic stack (Lisiecki and Raymo, 2005).

3.4 Glacial–interglacial $\delta^{18}O$ gradients across the Strait of Gibraltar

A compilation of the late Pliocene (3.33–2.60 Myrs) $\delta^{18}O$ records from the two studied sites are shown in Fig. 3 (Supplementary Table 1). Based on the average $\delta^{18}O$ values of glacial–interglacial MIS (see Supplementary Table 2), gradients between the corresponding stages in the Gulf of Cadiz (IODP Hole U1389E) and the Alboran Sea (ODP Hole 978A) have been established (Fig. 4-b) by a regression line that represents the slope of $\delta^{18}O$ per degree of longitude.

4 Results

4.1 Age model for the new $\delta^{18}O$ record of ODP 978A (369–337 mbsf)

The new $\delta^{18}O$ record from the upper part of ODP 978A is visually correlated to the Rossello section relying on established biostratigraphic tie points (Fig. 2-a; Table 1; Gradstein et al., 2012). As the upper part of both records is clearly delimited by the LO of *D. pentaradiatus* (2.52 Ma) and the lower part by the LO of *D. tamalis* (2.78 Ma) in ODP Site 978 and the FO of the foraminifer *N. atlantica* (sin) (2.72 Ma) in the Rossello Section, the first 0.06 Myrs in ODP 978A stay out of visual correlation to the Rosello section. ODP 978A ranges from 2.78 to 2.52 Ma which corresponds to 2.6 Ma in around 50 m of sediment core, therefore equivalent to 0.05 Ma/10 m. Accordingly, the visual correlation should start around 10 m topward from the LO of *D. tamalis* (2.78 Ma, 372.70 mbsf, Fig. 2-a). From that point (~362 mbsf), a similar number of $\delta^{18}O$ cycles can be observed on both records resulting in the best solution observed in Fig. 2-a. Our age model for OPD 978A indicates that the Pliocene/Pleistocene boundary at ~ 2.58 Ma is located at ~ 340 mbsf (Fig. 2-a). Sedimentation rates calculated for this interval vary from 0.06 to 0.57 m/ka (mean: 0.26 m/ka; Fig. 2-b).

4.2 Glacial/interglacial $\delta^{18}O$ gradients

$\delta^{18}O$ values for intervals I to III are shown vs. longitude in Fig. 3. IODP Hole U1389E suffers from notable gaps throughout the studied interval due to poor core recovery (Fig., 3; Stow et al., 2013; Grunert et al., 2017). For this reason, the section is subdivided into three well recovered intervals with continuous $\delta^{18}O$ records which will be in the focus of our study (Interval I: 3.33–3.27 Myrs; Interval II: 3.02–2.88 Myrs; Interval III: 2.73–2.60 Myrs; Figs. 3, 4-a).

In Interval I (3.33–3.27 Myrs), mean $\delta^{18}O$ values of IODP U1389E (Min: - 1.22 ‰; Max: + 0.46 ‰; Mean: - 0.34 ‰) and ODP 978A (Min: - 1.34 ‰; Max: + 0.49 ‰; Mean: - 0.39 ‰) are close to each other (Fig. 4-a1; Table 2). $\delta^{18}O$ gradients between ODP 978A and IODP U1389E change direction from interglacial MIS MG1 to glacial MIS M2 (Figs. 4-a1, 4-b1). $\delta^{18}O$ data from interglacial MIS MG1 reveals higher values in the Gulf of Cadiz compared to the Alboran Sea resulting in an isotopic gradient of - 0.08 ‰ degree^{-1}. In contrast, glacial period MIS M2 shows an opposite isotopic gradient ranging from + 0.05 to + 0.09 ‰ degree^{-1} for the two intermittent $\delta^{18}O$ maxima M2.1 and M2.2, respectively (Fig. 4-b1).

In Interval II (3.02–2.88 Myrs), mean $\delta^{18}O$ values of IODP U1389E (Min: - 0.99 ‰; Max: + 0.98 ‰; Mean: - 0.16 ‰) are considerably heavier compared to ODP 978A (Min: - 1.64 ‰; Max: + 0.50 ‰; Mean: - 0.50 ‰) (Fig., 4-a2; Table 2). The records are particularly well separated during $\delta^{18}O$ minima whereas they converge during maxima (Fig. 4-a2). Interglacial periods MIS G21, G19 and G15 and glacial periods MIS G22, G20 and G16 show isotopic gradients ranging from - 0.06 to - 0.13 ‰ degree^{-1} and - 0.04 to - 0.12 ‰ degree^{-1}, respectively (Fig. 4-b2). The only exception occurs during glacial period MIS G14 which shows a positive and relatively flat gradient of + 0.03 ‰ degree^{-1}.

In Interval III (2.73–2.60 Myrs), mean $\delta^{18}O$ values are again closer to each other (IODP U1389E: Min: - 0.85 ‰; Max: + 0.70 ‰; Mean: - 0.05 ‰ and ODP 978A: Min: - 1.11 ‰; Max: + 0.54 ‰; Mean: - 0.20 ‰) (Fig. 4-a3, Table 2). A wide range of $\delta^{18}O$ gradients has been calculated for Interval III (Fig. 4-b3). Interglacial periods MIS G7, G5 and G3 as well as glacial period MIS G4 show negative $\delta^{18}O$ gradients between - 0.03 and - 0.10 ‰ degree^{-1}). In contrast, glacial periods MIS G6, G2 and 104 reveal positive $\delta^{18}O$ gradients ranging from + 0.02 to + 0.06 ‰ degree^{-1} (Fig. 4-b3).

5 Discussion

5.1 Direction of $\delta^{18}O$ gradients

Our late Pliocene data set is based on the planktonic *Gs. ruber*, yet recent $\delta^{18}O$ gradients between the Gulf of Cadiz and the Alboran Sea have been established from the planktonic *Globigerina bulloides* (e.g. Cacho et al., 2001; Rogerson et al., 2010). A seasonal $\delta^{18}O$ offset between *Gs. ruber* (blooming in spring-summer) and *G. bulloides* (fall-winter) is evident from core top and parallel down core records of $\delta^{18}O$ in the late Quaternary (Figs. 5-a, 5-b; Voelker et al., 2009). However, despite this offset, the $\delta^{18}O$ gradients obtained from both species (*G. bulloides*: Rogerson et al., 2010; *Gs. ruber*: Rohling, 1999 and Salgueiro et al., 2008) show the same gradient direction with lighter $\delta^{18}O$ values in the Gulf of Cadiz and heavier values in the Alboran Sea (Fig. 5-b). Previous studies further show that the direction of this W-E gradient has not changed over the last ~25,000 years (Cacho et al., 2001; Rogerson et al., 2010). For the late Pliocene, however, our data suggest that the $\delta^{18}O$ gradient was considerably more variable, particularly during glacial stages (Figs. 4-a, 4-b). While all studied interglacial stages and glacial stages G22–G16 (except G14) of Interval II show a reversed gradient with respect to the present, the strong glacials M2, G14, G6, G2 and 104 show a gradient in line with present-day observations (Figs. 4-b, 5b).

Seasonal variations of Atlantic inflow reported in previous studies (e.g. Bormans et al., 1986; Ovchinnikov, 1974; Parada and Cantón, 1998; Vargas-Yáñez et al., 2002) can be the cause of Sea Surface Salinity (SSS) and Sea Surface Temperature (SST) variability. While seasonal changes of SSS are < 0.5, SST variability is more prominent and may result in brief temporary reversals of SST gradients (MEDATLAS, 2002; Rogerson et al., 2010). The Alboran Sea shows colder temperatures than the Gulf of Cadiz during all seasons due to upwelling, with occasional exceptions in summer under the influence of easterly winds (Bakun and Agostini, 2001; Folkard et al., 1997; Peeters et al., 2002; Rogerson et al., 2010; Sarhan et al., 2000; Shaltout and Omstedt, 2014). The $\delta^{18}O$ composition of present-day seawater is thus considered to be largely determined by changes of SST (Rogerson et al., 2010).

Reversed gradients in the late Pliocene could imply a different SST gradient due to a different current regime and/or lack of upwelling in the Alboran Sea in the Pliocene. Unfortunately, there is little data on SST available from the late Pliocene which would allow further evaluation. Khélifi et al. (2014) provide an alkenone-based SST record from ODP 978A from ~3.6 to 2.7 Myrs (Intervals I and II of this study) which indicates SSTs ranging from ~ 26.5 to 27.5 °C. A comparable alkenone-based SST reconstruction is

available from IODP Site U1387 in the Gulf of Cadiz and suggests an SST-range from ~ 26 to 27 °C from ~6 to 2.7 Myrs (Tzanova and Herbert, 2015). The comparison thus suggests that the difference in SST between the two sites was little to none, with surface waters in the Gulf of Cadiz probably slightly colder than in the Alboran Sea. Given a temperature sensitivity of ~ 0.23 ‰ °C^{-1} for planktonic foraminifera (O'Neill et al., 1969), estimated SST offsets cannot fully explain $\delta^{18}O$ gradients < -0.05 ‰ degree^{-1} in our case.

Variations of $\delta^{18}O$ gradients between the Mediterranean and Atlantic have also been explored in modeling studies by Rohling (1999). This model indicates that the direction of the gradient is largely influenced by relative humidity in the Mediterranean. While relative humidity values similar to present-day (which also persisted during the LGM; Rohling, 1999; cf. Rogerson et al., 2010) recreate $\delta^{18}O$ gradients as observed in Holocene and late Pleistocene foraminiferal records accurately, an increase of 5% in relative humidity is sufficient to reverse the $\delta^{18}O$ gradient due to isotopic depletion in the Mediterranean (Rohling, 1999). Pollen-based data suggest that annual precipitation and humidity in the Mediterranean were considerably higher relative to present-day levels during most of the late Pliocene with the exception of the strong glacial periods M2, G22, and G6–104 (Bertini, 2010; Fauquette et al., 1998; 1999; 2007). A warmer and more humid climate implies higher runoff and freshening of the Mediterranean surface waters leading to depleted $\delta^{18}O$ records as reported from Pliocene to Holocene data and models in previous studies (e.g. Gudjonsson and van der Zwaan, 1985; Kaboth et al., 2017; Thunell and Williams, 1989; Tindall and Haywood, 2015; Van Os et al., 1994; Vergnaud-Grazzini et al., 1977). We thus consider $\delta^{18}O$ depletion of Mediterranean waters during a warm and humid paleoclimate as the most likely explanation for the reversed gradients observed for interglacial stages from all three studied intervals as well as for the comparably warm glacial periods MIS G22, G20, G16, and G4 (Fig. 4-b). Conversely, arid conditions are indicated by pollen data only for the strong glacial stages M2, G6, G2, and 104 which herald increasing Northern Hemisphere Glaciation and for which our data suggest $\delta^{18}O$ gradients similar to the present (Fauquette et al., 1998; Figs. 4-b, 5-b).

5.2 Steepness of $\delta^{18}O$ gradients

While humidity likely explains variations of normal and reversed $\delta^{18}O$ gradients in the late Pliocene relative to the present-day trend, slope steepness is considered sensitive to the strength of surface water exchange across the Strait of Gibraltar (Rohling, 1999; Rogerson et al., 2010). On the basis of the previous statement, flat gradients are indicative of well-connected basins and enhanced exchange

whereas steeper gradients suggest more restricted conditions and reduced exchange (Rogerson et al., 2010).

The steepness of present-day gradients varies from 0.05 to 0.13 ‰ degree^{-1} depending on the time of calcification of *Gs. ruber* and *G. bulloides* (Fig. 5-b; this study; Rogerson et al., 2010; see chapter 5.1). In addition, Rogerson et al. (2010) reported a gradient of 0.26 ‰ degree^{-1} during the Last Glacial Maximum and of 0.01 and 0.14 ‰ degree^{-1} during Heinrich Stadials 1 and 2, respectively. Regardless of the direction, the steepness of late Pliocene slopes ranges from 0.05 to 0.13 ‰ degree^{-1} in all interglacial stages (except MIS G5) and glacial stages M2, G20, G16, and 104 (Fig. 4-b), thus indicating exchange rates which are similar or reduced to present-day values. In contrast, flatter gradients during glacial stages MIS G22, G14, G6, and G2 (0.02 to 0.04 ‰ degree^{-1}; Figs. 4-b2, 4-b3) point to enhanced exchange during these cold periods.

Support for our interpretation comes from available studies on MOW development during the late Pliocene to which the strength of AMOC is directly linked. The onset of long-term intensification of MOW has been linked to arid conditions during glacial stage M2, a second pulse of MOW occurs at ~ 2.8-2.7 (Grunert et al., 2017; Hernández-Molina et al., 2014; Khélifi et al., 2009; 2014; Sarnthein et al., 2017). Both pulses occur during these glacial periods in which we observe gradients similar to today and their succession is reflected in a flattening of gradients with the onset of NHG (~ 2.9 Ma) due to arid and cold conditions. Fluctuations of MOW intensity in the late Pliocene is in turn linked to global climate processes. Kleiven et al. (2002) demonstrated that lowered values of benthic δ^{13}C in the North Atlantic during glacial stages (MIS M2, G22, G16, G6–104 of our study) were related to a decreased production of North Atlantic Deep Water (NADW; Fig. 4-a) at high latitudes. Furthermore, periods of reduced Atlantic Meridional Overturning Circulation are linked to freshening of surface waters in the North Atlantic due to the increased iceberg melting and influx of ice-rafted debris (IRD) (Kleiven et al., 2002). Despite a strong influx of IRD is recorded at northern latitudes during MIS M2, the first occurrence of IRD at low mid-latitudes is recorded during G14 in samples from Deep Sea Drilling Program (DSDP) Site 607, located on the western flank of the Mid-Atlantic Ridge, with following peaks during glacials G6–104 (Bailey et al., 2010; Kleiven et al., 2002; Fig. 4-a). Thus, enhanced Mediterranean–Atlantic exchange suggested for MIS M2 parallels a drop of NADW production and weakened AMOC (DeSchepper et al., 2009; Khélifi et al., 2014; Sarnthein et al., 2017). Continuous occurrences of IRD at low mid-latitudes and reduced AMOC during glacial periods G14 to 104 fall together with intensified Mediterranean–Atlantic exchange during

strong glacial periods at the onset of the NHG. In contrast, the lack of IRD and increased $\delta^{13}C$ observed during interglacials (Kleiven et al., 2002) is in accordance with more restricted exchange during MIS MG1, G21, G19, G15, G5, and G3 (Fig. 4-a).The observed negative feedback between AMOC and Mediterranean–Atlantic exchange at the onset of the NHG seems to work similarly as during Heinrich Stadials from the Holocene as reported by Rogerson et al. (2010). However, higher resolution of our Pliocene records would be necessary to establish an accurate assessment of the timing of these feedback mechanisms within the glacial periods.

6 Conclusions

Late Pliocene $\delta^{18}O$ gradients of the planktonic foraminifer *Globigerinoides ruber* from IODP Hole U1389E (Gulf of Cadiz) and ODP Hole 978A (Alboran Sea) allowed the reconstruction of Mediterranean–Atlantic exchange variations between 3.33 and 2.60 Myrs, spanning the transition from the Mid-Pliocene Warm Period (MPWP) into the Northern Hemisphere Glaciation (NHG). The $\delta^{18}O$ gradients across the Strait of Gibraltar have been analyzed for individual glacial and interglacial stages in terms of direction and steepness.

In contrast to positive gradients in the present-day, elevated levels of humidity during the MPWP caused reversed and steep $\delta^{18}O$ gradients in the late Pliocene, especially during interglacial stages. Increased aridity caused a shift to positive gradients during strong glacial periods at Marine Isotope Stage (MIS) M2 and the onset of the NHG (MIS G22, G14, G2–104). Flat slopes indicate enhanced inflow during those cold and arid periods.

Intensified Mediterranean Outflow Water (MOW) has been reported during M2 and from 2.8 Ma coinciding with intense glacial stages. Strengthened Mediterranean–Atlantic exchange occurs at times of reduced Atlantic Meridional Overturning Circulation (AMOC) and North Atlantic Deep-water Formation (NADW) formation, when a higher influx of IRD arrived to lower latitudes causing the freshening of Atlantic surface waters. Our results thus suggest a negative feedback between AMOC and exchange rates at the Strait of Gibraltar in the late Pliocene as it has been proposed for the late Quaternary.

Data availability. Data will be archived at PANGAEA, data publisher for Earth and Environmental Science.

Competing interests. The authors declare that they have no conflict of interest.

Acknowledgments. This project is funded by the Austrian Science Fund (FWF; project P25831-N29). We thank the Expedition 339 from the Integrated Ocean Discovery Program for providing the samples used in this study. The Bremen Core Repository is acknowledged for the sampling performed on sediment cores from ODP Leg 161. Michael Joachimski from GeoZentrum Nordbayern (Erlangen) is acknowledged for performing isotopic analyses. We thank the two anonymous reviewers whose comments/suggestions helped improve and clarify this manuscript.

Figure captions

Figure 1. Location of IODP Site U1389, ODP Site 978 and the Rossello section. AI: Atlantic Inflow; EAG: Eastern Atlantic Gyre; GoCSC: Gulf of Cadiz Slope Current; MAW: Modified Atlantic Water; MOW: Mediterranean Outflow Water; WAG: Western Atlantic Gyre. The map was generated with GeoMapApp (http://www.geomapapp.org), using the default basemap, Global Multi-Resolution Topography (GMRT) Synthesis (Ryan et al., 2009).

Figure 2. (a) Stratigraphic framework established for ODP Hole 978A record based on indicated biostratigraphic tie points (FO: first occurrence; LO: last occurrence) and visual correlation of the $\delta^{18}O$ record with the Rossello section (Lourens et al., 1996). **(b)** Calculated sedimentation rates.

Figure 3. $\delta^{18}O$ records of IODP Hole U1389E and ODP Hole 978A from 3.33 to 2.60 Myrs. Intervals I, II and III with continuous $\delta^{18}O$ records from both cores are indicated. Marine Isotopic Stages (MIS) have been identified from Lourens et al. (1996) and Khélifi et al. (2014).

Figure 4. (a) Details of $\delta^{18}O$ records of IODP Hole U1389E and ODP Hole 978A for Intervals I–III. Periods of lowered NADW and increased influx of IRD from DSDP Site 607 (Mid-Atlantic Ridge) reported in Kleiven et al. (2002) are indicated. **(b)** Calculated $\delta^{18}O$ gradients between the Gulf of Cadiz and the Alboran Sea for glacial and interglacial stages in Intervals I–III (see Supplementary Table 2).

Figure 5. (a) Comparison of Pleistocene $\delta^{18}O$ values of *Globigerina bulloides* and *Globigerinoides ruber* at sites MD99-2336 and -2339 in the Gulf of Cadiz (Voelker et al., 2009). **(b)** Recent $\delta^{18}O$ gradients of *Gs. ruber* between core-top samples from the Gulf of Cadiz (M39022-1; Salgueiro et al., 2008) and the Alboran Sea (stations KS82-30 and KS-82-31; Rohling, 1999). Red circles represent mean values of the respective data-sets, the red line denotes the gradient between both basins. For comparison, the gradient obtained from $\delta^{18}O$ composition of *G. bulloides* by Rogerson et al. (2010) has been added.

Table captions

Table 1. Biostratigraphic events of ODP Hole 978A (Comas et al., 1996) and the Rossello Section (Lourens et al., 1996) used for the establishment of age constraints of the upper ODP 978A (Fig. 2-a). FO: first occurrence; LO: last occurrence.

Table 2. Maximum, minimum, mean and standard deviation of $\delta^{18}O$ values of IODP Hole U1389E and ODP Hole 978A in the long term and within Intervals I, II, and III.

Supplements

Supplementary Table 1. $\delta^{18}O$ values of IODP Hole U1389E and ODP Hole 978A from 3.33 to 2.60 Myrs. Intervals I, II and III are indicated.

Supplementary Table 2. Mean and standard deviation of $\delta^{18}O$ values for the studied glacial and interglacial stages of Intervals I, II and III at IODP Hole U1389E and ODP Hole 978A (Fig. 3).

References

Ambar, I., & Howe, M.R. (1979). Observations of the Mediterranean outflow-I. Mixing the Mediterranean Outflow. Deep-Sea Res. 26, 535-554. doi:https://doi.org/10.1016/0198-0149(79)90095-5.

Backman, J., Raffi, I., Rio, D., Fornaciari, E., Pälike, H. (2012). Newsl. Stratigr. 45(3), 221-244.

Bahr, A., Kaboth, S., Jiménez-Espejo, F.J., Sierro, F.J., Voelker, A.H.L., Lourens, L., Röhl, U., Reichart, G.J., Escutia, C., Hernández-Molina, F.J., Pross, J., Friedrich, O. (2015). Persistent monsoonal forcing of

Mediterranean Outflow Water dynamics during the late Pleistocene. Geology 43 (11), 951-954. doi:10.1130/G37013.1.

Bailey, I, Bolton, C.T., DeConto, R.M., Pollard, D., Schiebel, R., & Wilson, P.A. (2009). A low threshold for North Atlantic ice rafting from "low-slung slippery" late Pliocene ice sheets. Paleoceanography, 25, PA1212. doi:10.1029/2009PA001736.

Bakun, A., Agostini, V.N. (2001). Seasonal patterns of wind-induced upwelling/downwelling in the Mediterranean Sea. Sci. Mar. 65 (3), 243-257. doi:http://dx.doi.org/10.3989/scimar.2001.65n3243.

Bartoli, G., Sarnthein, M., Weinelt, & M. (2006). Late Pliocene millennial-scale climate variability in the northern North Atlantic prior to and after the onset of Northern Hemisphere glaciation. Paleoceanography 21, PA4205. doi:10.1029/2005PA001185.

Bertini, A., 2010. Pliocene to Pleistocene palynoflora and vegetation in Italy: State of the art. Quatern. Int. 225, 5-24. doi:10.1016/j.quaint.2010.04.025.

Borenäs, K.M., Wåhlin, A.K., Ambar, I., & Serra, N. (2002).The Mediterranean outflow splitting—a comparison between theoretical models and CANIGO data. Deep-Sea Res. II 49, 4195–4205. doi:https://doi.org/10.1016/S0967-0645(02)00150-9.

Bormans, M., Garrett, C., & Thompson, R. (1986). Seasonal variability of the surface inflow through the Strait of Gibraltar. Oceanol. Acta 9 (4), 403–414. doi:http://archimer.ifremer.fr/doc/00110/22092/.

Bryden, H.L., & Kinder, T.H. (1991). Steady two-layer exchange through the Strait of Gibraltar. Deep-Sea Res. I 38 (1), S445-S463. doi:https://doi.org/10.1016/S0198-0149(12)80020-3.

Bryden, H.L., & Stommel, H.M. (1982). Origins of the Mediterranean Outflow. J. Mar. Res. 40, 55–71.

Bryden, H.L., Candela, J., & Kinder, T.H. (1994). Exchange through the Strait of Gibraltar. Progr. Oceanogr. 33, 201–248.

Budyko, M.I., Ronov, A.B., & Yanshin, A.L. (1985). The History of the Earth's Atmosphere. Leningrad, Gidrometeoirdat. 209 pp. (In Russian; English translation: Springer, Berlin, 1987,139 pp).

Bukry, D. (1973). Low-latitude coccolith biostratigraphic zonation. In: Edgar, N.T., Saunders, J. B., et al., Initial Reports DSDP 15, Washington (U.S. Govt. Printing Office), 685–703. doi:10.2973/dsdp.proc.15.116.1973.

Cacho, I., Grimalt, J.O., Canals, M., Sbaffi, L., Shackleton, N., Schönfeld, J., & Zahn, R. (2001). Variability of the western Mediterranean Sea surface temperature during the last 25,000 years and its connection with the northern hemisphere climatic changes. Paleoceanography 16, 40-52. doi:10.1029/2000PA000502.

Comas, M.C., Zahn, R., Klaus, A., et al., (1996). Proc. Ocean Drill. Prog.,, Initial Reports, v. 161: College Station, Texas, Ocean Drilling Program.

DeSchepper, S., Head, M.J., & Groeneveld, J. (2009). North Atlantic Current variability through marine isotope stage M2 (circa 3.3 Ma) during the mid-Pliocene. Paleoceanography 24: PA4206. doi:10.1029/2008PA001725.

Dowsett, H., M. Robinson, A. Haywood, U. Salzmann, D. Hill, L. Sohl, M. Chandler, M. Williams, K. Foley, D. Stoll (2010). The PRISM3D paleoenvironmental reconstruction. Stratigraphy 7 (2-3), 123-139.

Dowsett, H.J., Robinson, M.M., Haywood, A.M., Hill, D.J., Dolan, A.M., Stoll, D.K., Chan, W.L., Abe-Ouchi, A., Chandler, M.A., Rosenbloom, N.A., Otto-Bliesner, B.L., Bragg, F.J., Lunt, D.J., Foley, K.M., & Riesselman, C.R. (2012). Assessing confidence in Pliocene sea surface temperatures to evaluate predictive models. Nat. Clim. Change 2, 365–371. doi:10.1038/nclimate1455.

Fauquette, S., Guiot, J., & Suc, J.-P. (1998). A method for climatic reconstruction of the Mediterranean Pliocene using pollen data. Palaeogeogr. Palaeoclimatol. Palaeoecol. 144, 183-201. doi:https://doi.org/10.1016/S0031-0182(98)00083-2.

Fauquette, S., Suc, J.-P., Guiot, J., Diniz, F., Feddi, N., Zheng, Z., Bessais, E., Drivaliari, A. (1999). Climate and biomes in the West Mediterranean area during the Pliocene. Palaeogeogr. Palaeoclimatol. Palaeoecol. 152, 15-36.

Fauquette, S., Suc, J.-P., Jiménez-Moreno, G., Micheels, A., Jost, A., Favre, E., Bachiri-Taoufiq, N., Bertini, A., Clet-Pellerin, M., Diniz, F., Farjanel, G., Feddi, N., Zheng, Z. (2007). Latitudinal climatic gradients in the Western European and Mediterranean regions from the Mid-Miocene (c. 15 Ma) to the Mid-Pliocene (c. 3.5 Ma) as quantified from pollen data. In: Williams, M., Haywood, A. M., Gregory, F. J. & Schmidt, D. N. (eds). Deep-Time Perspectives on Climate Change: Marrying the Signal from Computer Models and Biological Proxies. The Micropalaeontological Society, Special Publications. The Geological Society, London, 481–502.

Folkard, A.M., Davies, P.A., Fiúza, A.F.G., & Ambar, I. (1997). Remotely sensed sea surface thermal patterns in the Gulf of Cadiz and the Strait of Gibraltar: Variability, correlations, and relationships with the surface wind field. J. Geophys. Res. 102 (C3), 5669-5683.

García, M., Hernández-Molina, F.J., Llave, E., Stow, D.A.V., León, R., Fernández-Puga, M.C., Díaz del Río, V., & Somoza, L. (2009). Contourite erosive features caused by the Mediterranean Outflow Water in the Gulf of Cadiz: quaternary tectonic and oceanographic implications. Mar. Geol. 257, 24–40. doi:http://dx.doi.org/10.1016/j.margeo.2008.10.009.

García-Gallardo, Á., Grunert, P., Van der Schee, M., Sierro, F.J., Jiménez-Espejo, F.J., Álvarez-Zarikian, C.A., & Piller, W.E. (2017). Benthic foraminifera-based reconstruction of the first Mediterranean–Atlantic exchange in the early Pliocene Gulf of Cadiz. Palaeogeogr. Palaeoclimatol. Palaeoecol. 472, 93-107. doi:10.1016/j.palaeo.2017.02.009.

Gascard, J.C., & Richez, C. (1985). Water masses and circulationin the western Alboran Sea and in the Strait of Gibraltar. Prog. Oceanogr. 15, 157-216. doi:https://doi.org/10.1016/0079-6611(85)90031-X.

Gradstein, F.M., Ogg, J.G., Hilgen, F.J. (2012). On the Geologic Time Scale. Newsl. Stratigr. 45 (2), 171-188. doi: 10.1127/0078-0421/2012/0020

Grunert, P., Balestra, B., Richter, C., Flores, J.A., Auer, G., García-Gallardo, Á., & Piller, W.E. (2017). Revised and refined age model for the upper Pliocene of IODP Site U1389 (IODP Expedition 339, Gulf of Cádiz). Newsl. Stratigr. doi: https://doi.org/10.1127/nos/2017/0396.

Gudjonsson, L., & van der Zwaan, G. J. (1985). Anoxic events in the Pliocene Mediterranean: Stable isotope evidence for run-off. Proc. K. Ned. Akad. Wet. Ser. B 88, 69-82.

Haywood, A.M., & Valdes, P.J. (2004). Modelling Pliocene warmth: contribution of atmosphere, oceans and cryosphere. Earth Planet. Sci. Letters 218 (3–4), 363-377. doi:https://doi.org/10.1016/S0012-821X(03)00685-X.

Hernández-Molina, F.J., Llave, E., Stow, D.A.V., García, M., Somoza, L., Vázquez, J.T., Lobo, F.J., Maestro, A., Díaz del Río, V., León, R., Medialdea, T., & Gardner, J. (2006). The contourite depositional system of the Gulf of Cádiz: a sedimentary model related to the bottom current activity of the Mediterranean outflow water and its interaction with the continental margin. Deep-Sea Res. II 53 (11–13), 1420–1463. doi:http://dx.doi.org/10.1016/j.dsr2.2006.04.016.

Hernández-Molina, F.J., Stow, D.A.V., Álvarez-Zarikian, C.A., Acton, G., Bahr, A., Balestra, B., Ducassou, E., Flood, R., Flores, J.-A., Furota, S., Grunert, P., Hodell, D., Jimenez-Espejo, F., Kim, J.K., Krissek, L., Kuroda, J., Li, B., Llave, E., Lofi, J., Lourens, L., Miller, M., Nanayama, F., Nishida, N., Richter, C., Roque, C., Pereira, H., Sanchez Goñi, M.F., Sierro, F.J., Singh, A.D., Sloss, C., Takashimizu, Y., Tzanova, A., Voelker, A., Williams, T., & Xuan, C. (2014). Onset of Mediterranean outflow into the North Atlantic. Science 344, 1244–1250. doi:10.1126/science.1251306.

Iorga, M.C., & Lozier, M.S. (1999). Signatures of the Mediterranean outflow from a North Atlantic climatology: 1. Salinity and density fields. J. Geophys. Res. 104 (11), 259-260. doi:10.1029/1999JC900115.

Ivanovic, R.F., Valdes, P.J., Gregoire, L., Flecker, R., Gutjahr, M. (2014). Sensitivity of modern climate to the presence, strength and salinity of Mediterranean–Atlantic exchange in a global general circulation model. Clim. Dyn. 42, 859-877. doi:10.1007/s00382-013-1680-5.

Kaboth, S., Bahr, A., Reichart, G.-J., Jacobs, B., & Lourens, L.J. (2016). New insights into upper MOW variability over the last 150kyr from IODP 339 Site U1386 in the Gulf of Cadiz. Mar. Geol. 377, 136-145. doi:10.1016/j.margeo.2015.08.014.

Kaboth, S., Grunert, P., & Lourens, L.J. (2017). Mediterranean Outflow Water variability during the Early Pleistocene climate transition. Clim. Past 13, 1023–1035. doi:https://doi.org/10.5194/cp-13-1023-2017.

Khélifi, N., Sarnthein, M., Andersen, N., Blanz, T., Frank, M., Garbe-Schönberg, D., Haley, B.A., Stumpf, R., & Weinelt, M. (2009). A major and long-term Pliocene intensification of the Mediterranean outflow, 3.5-3.3 Ma ago. Geology 37 (9), 811–814. doi:10.1130/G30058A.1.

Khélifi, N., Sarnthein, M., Frank, M., Andersen, N., & Garbe-Schönberg, D. (2014). Late Pliocene variations of the Mediterranean outflow. Mar. Geol. 357, 182–194. doi:10.1016/j.margeo.2014.07.006.

Kleiven, H.F., Jansen, E., Fronval, T., & Smith, T.M. (2002). Intensification of Northern Hemisphere glaciations in the circum Atlantic region (3.5–2.4 Ma)—ice-rafted detritus evidence. Palaeogeogr. Palaeoclimatol. Palaeoecol. 184, 213–223. doi:https://doi.org/10.1016/S0031-0182(01)00407-2.

Llave, E., Hernández-Molina, F.J., Somoza, L., Stow, D.A.V., & Díaz del Río, V. (2007). Quaternary evolution of the contourite depositional system in the Gulf of Cadiz. Geol. Soc. Spec. Publ. 276, 49-79. doi:10.1144/GSL.SP.2007.276.01.03.

Lisiecki, L.E., Raymo., M.E. (2005). A Pliocene-Pleistocene stack of 57 globally distributed benthic d18O records. Paleoceanography 20, PA 1003. doi:10.1029/2004PA001071.

Lourens, L.J., Hilgen, F.J., Gudjonsson, L., & Zachariasse, W.J. (1992). Late Pliocene to early Pleistocene astronomically forced sea surface productivity and temperature variations in the Mediterranean. Mar. Micropaleontol. 19, 49-78. doi:https://doi.org/10.1016/0377-8398(92)90021-B.

Lourens, L.J., Antonarakou, A., Hilgen, F.J., Van Hoof, A.A.M., Vergnaud-Grazzini, C., & Zachariasse, W.J. (1996). Evaluation of the Plio-Pleistocene astronomical timescale. Palaeoceanography 11 (4), 391-413. doi:10.1029/96PA01125.

Lunt, D.J., Haywood, A.M., Schmidt, G.A., Salzmann, U., Valdes, P.J., Dowsett, H.J., & Loptson, C.A. (2012). On the causes of mid-Pliocene warmth and polar amplification. Earth Planet. Sci. Lett. 321, 128–138. doi:https://doi.org/10.1016/j.epsl.2011.12.042.

Madelain, F. (1970). Influence de la topographie du fond sur l'écoulement méditerréen entre le Détroit de Gibraltar et le Cap Saint-Vincent. Cah. Océanograph. 22, 43-61.

Marchès, E., Mulder, T., Cremer, M., Bonnel, C., Hanquiez, V., Gonthier, E., & Lecroart, P. (2007). Contourite drift construction influenced by capture of Mediterranean outflow water deep-sea current by the Portimao submarine canyon (Gulf of Cadiz, south Portugal). Mar. Geol. 242, 247–260. doi:https://doi.org/10.1016/j.margeo.2007.03.013.

MEDATLAS, (2002), MEDATLAS/2002 database. Mediterranean and Black Sea database of temperature salinity and biochemical parameters. Climatological Atlas: IFREMER Edition, MEDAR Group, Issy-les-Moulineaux, France.

Millot, C. (1999). Circulation in the Western Mediterranean Sea. J. Marine Syst. 20 (1-4), 423-442. doi:https://doi.org/10.1016/S0924-7963(98)00078-5.

Millot, C. (2013). Levantine Intermediate Water characteristics: an astounding general misunderstanding! Sci. Mar. 77 (2), 237-232. doi:10.3989/scimar.03518.13A.

Minas, H., Coste, J.B., Le Corre, P., Minas, M., & Raimbault, P. (1991). Biological and geochemical signatures associated with the water circulation through the Straits of Gibraltar and in the western Alboran Sea. J. Geophys. Res. 96 (C5), 8755-8771. doi:10.1029/91JC00360.

Ochoa, J., & Bray, N.A. (1991). Water mass exchange in the Gulf of Cadiz. Deep-Sea Res. I 38. 465. doi:http://dx.doi.org/10.1016/S0198-0149(12)80021-5.

O'Neil, J.R., Clayton, R.N., & Mayeda, T.K. (1969). Oxygen isotope fractionation on divalent metal carbonates. J. Chem. Phys. 51, 5547–5558. doi:10.1063/1.1671982.

Ovchinnikov, I.M. (1974). On the water balance of the Mediterranean Sea. Oceanology 14, 198– 202.

Pagani, M., Liu, Z., LaRiviere, L., & Ravelo, A.C. (2010). High Earth-system climate sensitivity determined from Pliocene carbon dioxide concentrations. Nat. Geosci. 3, 27–30. doi:10.1038/ngeo724.

Parada, M., & Cantón, M. (1998). The spatial and temporal evolution of thermal structures in the Alboran Sea Mediterranean basin. Int. J. Remote Sens. 19 (11), 2119– 2131. doi:http://dx.doi.org/10.1080/014311698214901.

Peeters, F.J.C., Brummer, G.-J.A., & Ganssen, G. (2002). The effect of upwelling on the distribution and stable isotope composition of *Globigerina bulloides* and *Globigerinoides ruber* (planktic foraminifera) in modern surface waters of the NW Arabian Sea. Glob. Planet. Change 34, 269-291. doi:https://doi.org/10.1016/S0921-8181(02)00120-0.

Peliz, A., Marchesiello, P., Santos, A.M.P., Dubert, J., Teles-Machado, A., Marta-Almeida, M., Le Cann, B. (2009). Surface circulation in the Gulf of Cadiz: 2. Inflow-outflow coupling and the Gulf of Cadiz slope current. J. Geophys. Res. 114, C03011. doi:10.1029/2008JC004771.

Raymo, M.E., Grant, B., Horowitz, M., & Rau, G.H. (1996). Mid-Pliocene warmth: stronger greenhouse and stronger conveyor. Mar. Micropaleontol. 27, 313–326. doi:https://doi.org/10.1016/0377-8398(95)00048-8.

Reid, J.L. (1979). On the contribution of the Mediterranean Sea outflow to the Norwegian–Greenland Sea. Deep-Sea Res. 26, 1199–1223. doi:10.1016/0198-0149(79)90064-5.

Rhein, M. (1995). Deep water formation in the Western Mediterranean. J. Geophys. Res. 10 (C4), 6943-6959. doi:10.1029/94JC03198.

Robinson, M.M., Dowsett, H.J., & Chandler, M.A. (2008). Pliocene Role in Assessing Future Climate Impacts. Eos 89 (49), 501-502. doi:10.1029/2008EO490001.

Rogerson, M., Colmenero-Hidalgo, E., Levine, R.C., Rohling, E.J., Voelker, A.H.L., Bigg, G.R., Schönfeld, J., & Garrick, K. (2010). Enhanced Mediterranean–Atlantic exchange during Atlantic freshening phases. Geochem. Geophy. Geosy. 11, Q08013. doi:10.1029/2009GC002931.

Rogerson, M., Rohling, E.J., Bigg, G.R., & Ramirez, J. (2012). Paleoceanography of the Atlantic-Mediterranean exchange: overview and first quantitative assessment of climatic forcing. Rev. Geophys. 50 (2), RG2003. doi:10.1029/2011RG000376.

Rohling, E.J. (1999). Environmental control on Mediterranean salinity and $\delta^{18}O$. Paleoceanography 14 (6), 706-715. doi:10.1029/1999PA900042.

Ryan, W.B.F., Carbotte, S.M., Coplan, J.O., O'Hara, S., Melkonian, A., Arko, R., Weissel, R.A., Ferrini, V., Goodwillie, A., Nitsche, F., Bonczkowski, J., & Zemsky, R. (2009). Global multi-resolution topography synthesis. Geochem. Geophy. Geosy. 10, Q03014. doi:http://dx.doi.org/10.1029/2008GC002332.

Salgueiro, E., Voelker, A.H.L., Abrantes, F., Meggers, H., Pflaumann, U., Lončarić, N., González-Álvarez, R., Oliveira, P., Bartels-Jónsdóttir, H.B., Moreno, J., & Wefer, G. (2008). Planktonic foraminifera from modern sediments reflect upwelling patterns off Iberia: Insights from a regional transfer function. Mar. Micropaleontol. 66, 135-164. doi:10.1016/j.marmicro.2007.09.003.

Sarhan, T., García-Lafuente, J., Vargas, M., Vargas, J.M., & Plaza, F. (2000). Upwelling mechanisms in the northwestern Alboran Sea. J. Marine Sys. 23, 317-331. doi:https://doi.org/10.1016/S0924-7963(99)00068-8.

Sarnthein, M., Grunert, P., Khélifi, N., Frank, M., & Nürnberg, D. (2017). Interhemispheric teleconnections: Late Pliocene change in Mediterranean outflow water linked to changes in Indonesian Through‐Flow and Atlantic Meridional Overturning Circulation, a review and update. Int. J. Earth Sci. doi:https://doi.org/10.1007/s00531-017-1505-6.

Seki, O., Foster, G.L., Schmidt, D.N., Mackensen, A., Kawamura, K., & Pancost, R.D. (2010). Alkenone and boron-based Pliocene pCO2 records. Earth Planet. Sci. Lett. 292, 201–211. doi:https://doi.org/10.1016/j.epsl.2010.01.037.

Serra, N., Ambar, I., & Käse, R.H. (2005). Observations and numerical modeling of the Mediterranean outflow splitting and eddy generation. Deep-Sea Res. II 52, 383–408. doi:https://doi.org/10.1016/j.dsr2.2004.05.025.

Shaltout, M., & Omstedt, A. (2014). Recent sea surface temperature trends and future scenarios for the Mediterranean Sea. Oceanologia 56 (3), 411-443. doi:https://doi.org/10.5697/oc.56-3.411.

Stow, D.A.V., Hernández-Molina, F.J., & Alvarez-Zarikian, C. (2013). Expedition 339 summary. Proc. Ocean Drill. Prog. doi:http://dx.doi.org/10.2204/iodp.proc.339.104.2013.

Thunell, R.C., & Williams, D.F. (1989). Glacial-Holocene changes in the Mediterranean Sea: hydrographic and depositional effects. Nature 338, 493-496.

Tindall, J.C., Haywood, A.M. (2015). Modeling oxygen isotopes in the Pliocene:Large-scale features over the land and ocean. Paleoceanography 30, 1183-1201. doi:10.1002/2014PA002774.

Tzanova, A., & Herbert, T. (2015). Regional and global significance of Pliocene sea surface temperatures from the Gulf of Cadiz (Site U1387) and the Mediterranean. Glob. Planet. Change 133, 371-377. doi:http://dx.doi.org/10.1016/j.gloplacha.2015.07.001.

Van der Schee, M., Sierro, F.J., Jiménez-Espejo, F.J., Hernández-Molina, F.J., Flecker, R., Flores, J.A., Acton, G., Gutjahr, M., Grunert, P., García-Gallardo., Á., & Andersen, N. (2016). Evidence of early bottom water current flow after the Messinian Salinity Crisis in the Gulf of Cadiz. Mar. Geol. 380, 315–329. doi:http://dx.doi.org/10.1016/j.margeo.2016.04.005.

Van Os, B.J.H., Lourens, L.J., Hilgen, F.J., & De Lange, G.J. (1994). The Formation of Pliocene sapropels and carbonate cycles in the Mediterranean: Diagenesis, dilution, and productivity. Paleoceanography 9 (4), 601-617. doi:10.1029/94PA00597.

Vargas-Yáñez, M., Plaza, F., García-Lafuente, J., Sarhan, T., Vargas, J.M., & Vélez-Belchi, P. (2002). About the seasonal variability of the Alboran Sea circulation. J. Marine Syst. 35, 229-248. doi:https://doi.org/10.1016/S0924-7963(02)00128-8.

Vergnaud-Grazzini, C., Ryan, W.B.F., & Cita, M.B. (1977). Stable isotope fractionation, climatic change and episodic stagnation in the eastern Mediterranean during the late Quaternary. Mar. Micropaleontol. 2, 353–370. doi:https://doi.org/10.1016/0377-8398(77)90017-2.

Voelker, A.H.L., Lebreiro, S.M., Schönfeld, J., Cacho, I., Erlenkeuser, H., & Abrantes, F. (2006). Mediterranean outflow strengthening during northern hemisphere coolings: A salt source for the glacial Atlantic? Earth Planet. Sci. Lett. 245, 39–55. doi:https://doi.org/10.1016/j.epsl.2006.03.014.

Voelker, A.H.L., Schönfeld, J., Erlenkeuser, H., & Abrantes, F. (2009). Hydrographic conditions along the western Iberian margin during marine isotope stage 2. Geochem. Geophy. Geosy. 10 (12), Q12U08. doi:10.1029/2009GC002605.

Voelker, A.H.L., Salgueiro, E., Rodrigues, T., Jiménez-Espejo, F.J., Bahr, A., Alberto, A., Loureiro, I., Padilha, M., Rebotim, A., & Röhl, U. (2015). Mediterranean outflow and surface water variability off southern Portugal during the early Pleistocene: a snapshot at marine isotope stages 29 to 34 (1020–1135 ka). Glob. Planet. Change 133, 223–237. doi:10.1016/j.gloplacha.2015.08.015.

Wüst, G. (1961). On the vertical circulation of the Mediterranean Sea. J. Geophys. Res. 66, 3261-3271. doi:10.1029/JZ066i010p03261.

Zenk, W. (1975). On the Mediterranean outflow west of Gibraltar. Meteor-Forschungsergebnisse A (16), 23-34.

Table 1

ODP Hole 978A	**Biostratigraphic event**	**Depth (mbsf)**	**Age (Ma)**
	LO *D. pentaradiatus*	323.74	2.52
	LO *D. tamalis*	372.70	2.78
Rossello Section	**Biostratigraphic event**	**Position sedimentary cycles (m)**	**Age (Ma)**
	LO *D. pentaradiatus*	138.05	2.51
	LO *D. surculus*	135.05	2.55
	FO *N. atlantica* (sin)	83.53	2.72

605 **Table 2**

Period	**Long term (3.33-2.60 Myrs)**		**Short terms**					
			Interval I (2.73-2.60 Myrs)		**Interval II (3.02-2.88 Myrs)**		**Interval III (3.33-3.27 Myrs)**	
Site ID	**IODP Hole U1389E**	**ODP Hole 978A**	**IODP Hole U1389E**	**ODP Hole 978A**	**IODP Hole U1389E**	**ODP Hole 978A**	**IODP Hole U1389E**	**ODP Hole 978A**
Min	-1.22	-1.81	-1.22	-1.34	-0.99	-1.64	-0.85	-1.11
Max	0.98	0.68	0.46	0.49	0.98	0.5	0.7	0.54
Average	-0.14	-0.41	-0.34	-0.39	-0.16	-0.5	-0.05	-0.2
SD	0.37	0.51	0.38	0.52	0.39	0.54	0.31	0.44

Figure 1

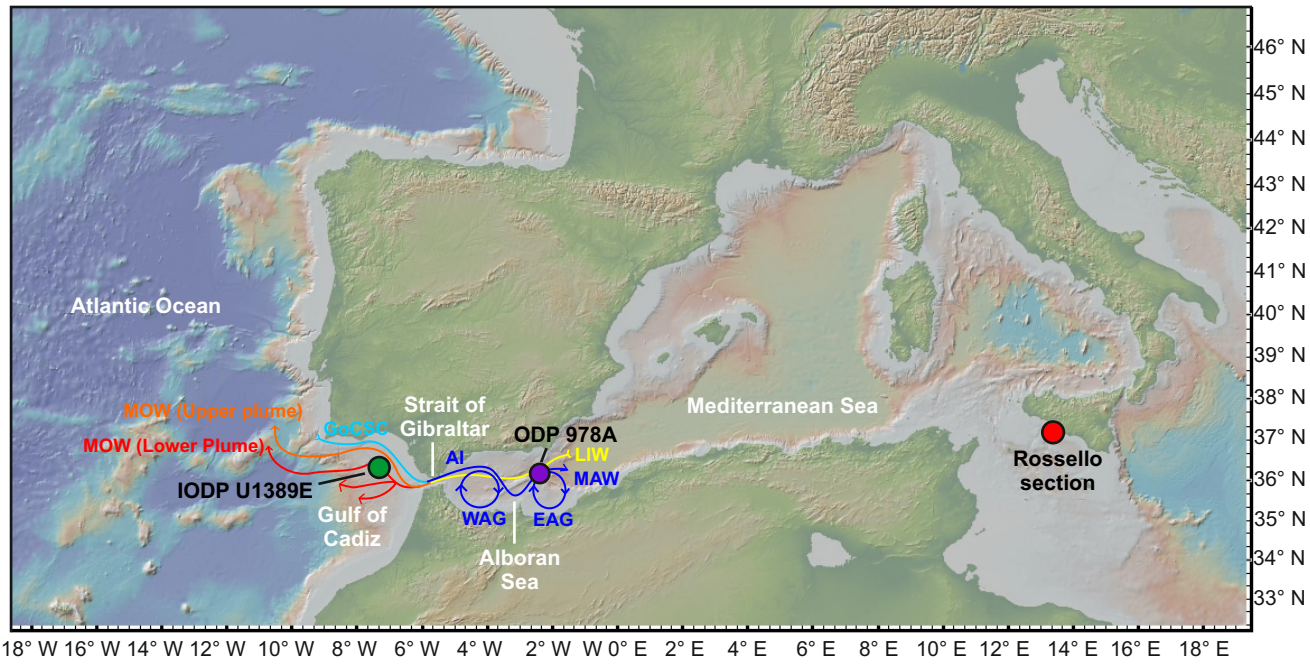
Atlantic Ocean
MOW (Upper plume)
MOW (Lower Plume)
GoCSC
Strait of Gibraltar
AI
ODP 978A
LIW
MAW
IODP U1389E
Gulf of Cadiz
WAG
EAG
Alboran Sea
Mediterranean Sea
Rossello section
46° N
45° N
44° N
43° N
42° N
41° N
40° N
39° N
38° N
37° N
36° N
35° N
34° N
33° N
18° W 16° W 14° W 12° W 10° W 8° W 6° W 4° W 2° W W 0° E 2° E 4° E 6° E 8° E 10° E 12° E 14° E 16° E 18° E

Figure 2

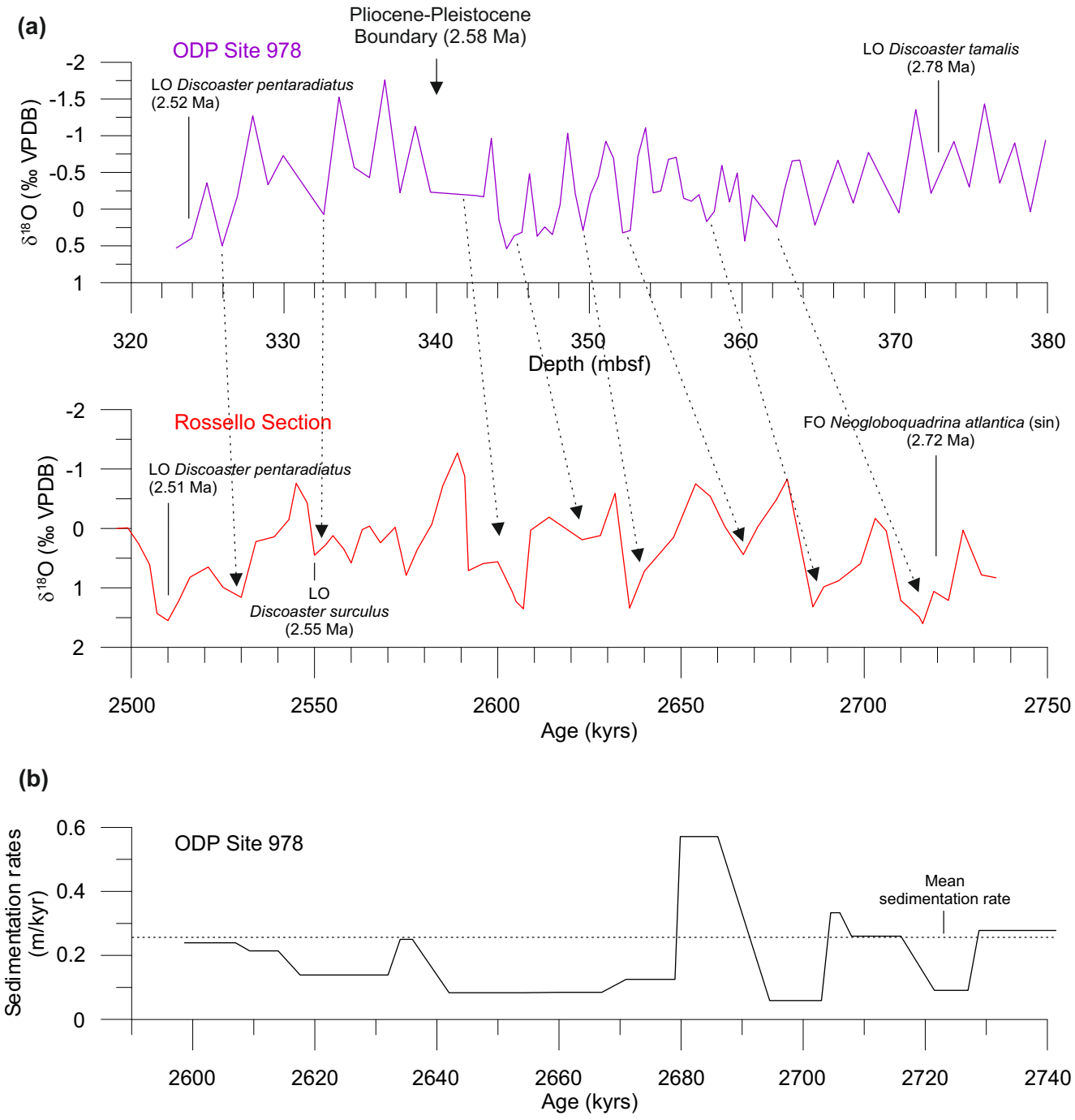
(a)
ODP Site 978
Pliocene-Pleistocene
Boundary (2.58 Ma)
LO Discoaster pentaradiatus
(2.52 Ma)
LO Discoaster tamalis
(2.78 Ma)
δ18O (‰ VPDB)
-2
-1.5
-1
-0.5
0
0.5
1
320
330
340
350
360
370
380
Depth (mbsf)
Rossello Section
LO Discoaster pentaradiatus
(2.51 Ma)
FO Neogloboquadrina atlantica (sin)
(2.72 Ma)
LO
Discoaster surculus
(2.55 Ma)
δ18O (‰ VPDB)
-2
-1
0
1
2
2500
2550
2600
2650
2700
2750
Age (kyrs)
(b)
ODP Site 978
Mean
sedimentation rate
Sedimentation rates
(m/kyr)
0.6
0.4
0.2
0
2600
2620
2640
2660
2680
2700
2720
2740
Age (kyrs)

Figure 3

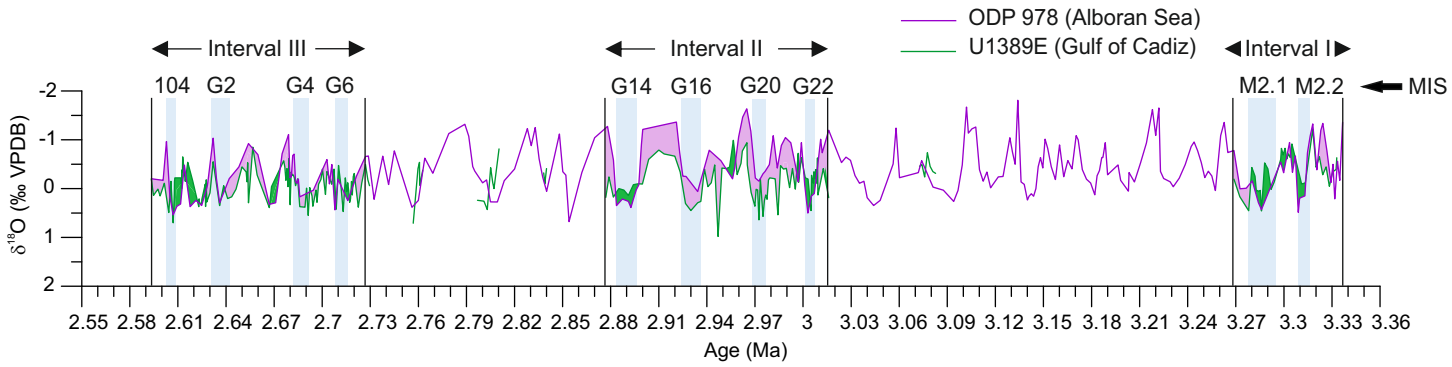
ODP 978 (Alboran Sea)
U1389E (Gulf of Cadiz)
Interval III
Interval II
Interval I
104
G2
G4
G6
G14
G16
G20
G22
M2.1
M2.2
MIS
δ18O (‰ VPDB)
-2
-1
0
1
2
2.55 2.58 2.61 2.64 2.67 2.7 2.73 2.76 2.79 2.82 2.85 2.88 2.91 2.94 2.97 3 3.03 3.06 3.09 3.12 3.15 3.18 3.21 3.24 3.27 3.3 3.33 3.36
Age (Ma)

Figure 4

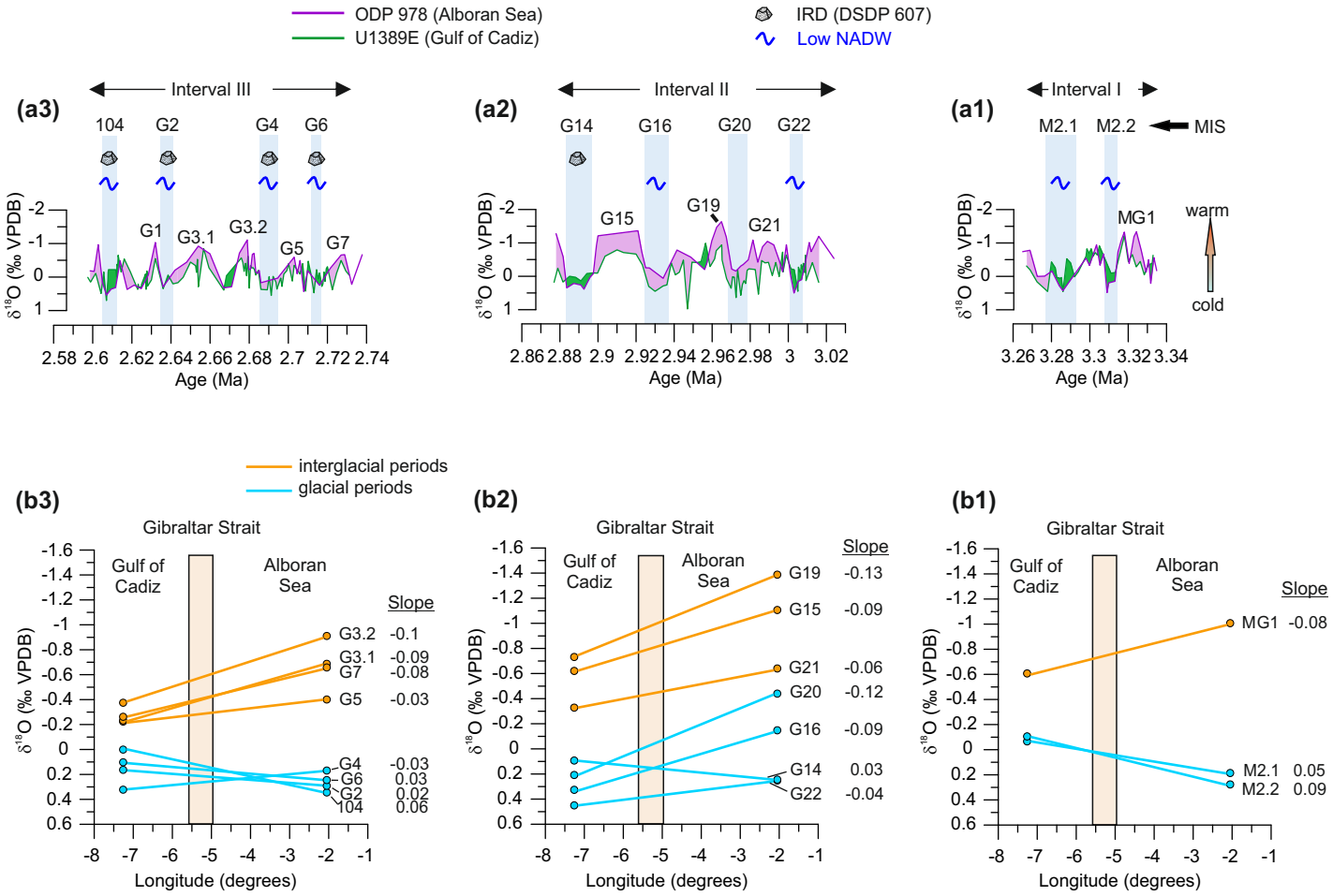
ODP 978 (Alboran Sea)
U1389E (Gulf of Cadiz)
IRD (DSDP 607)
Low NADW
(a3)
Interval III
104
G2
G4
G6
G1
G3.1
G3.2
G5
G7
δ18O (‰ VPDB)
Age (Ma)
(a2)
Interval II
G14
G16
G20
G22
G15
G19
G21
(a1)
Interval I
M2.1
M2.2
MIS
MG1
warm
cold
interglacial periods
glacial periods
(b3)
Gibraltar Strait
Gulf of Cadiz
Alboran Sea
Slope
G3.2 -0.1
G3.1 -0.09
G7 -0.08
G5 -0.03
G4 -0.03
G6 0.03
G2 0.02
104 0.06
Longitude (degrees)
(b2)
G19 -0.13
G15 -0.09
G21 -0.06
G20 -0.12
G16 -0.09
G14 0.03
G22 -0.04
(b1)
MG1 -0.08
M2.1 0.05
M2.2 0.09

Figure 5

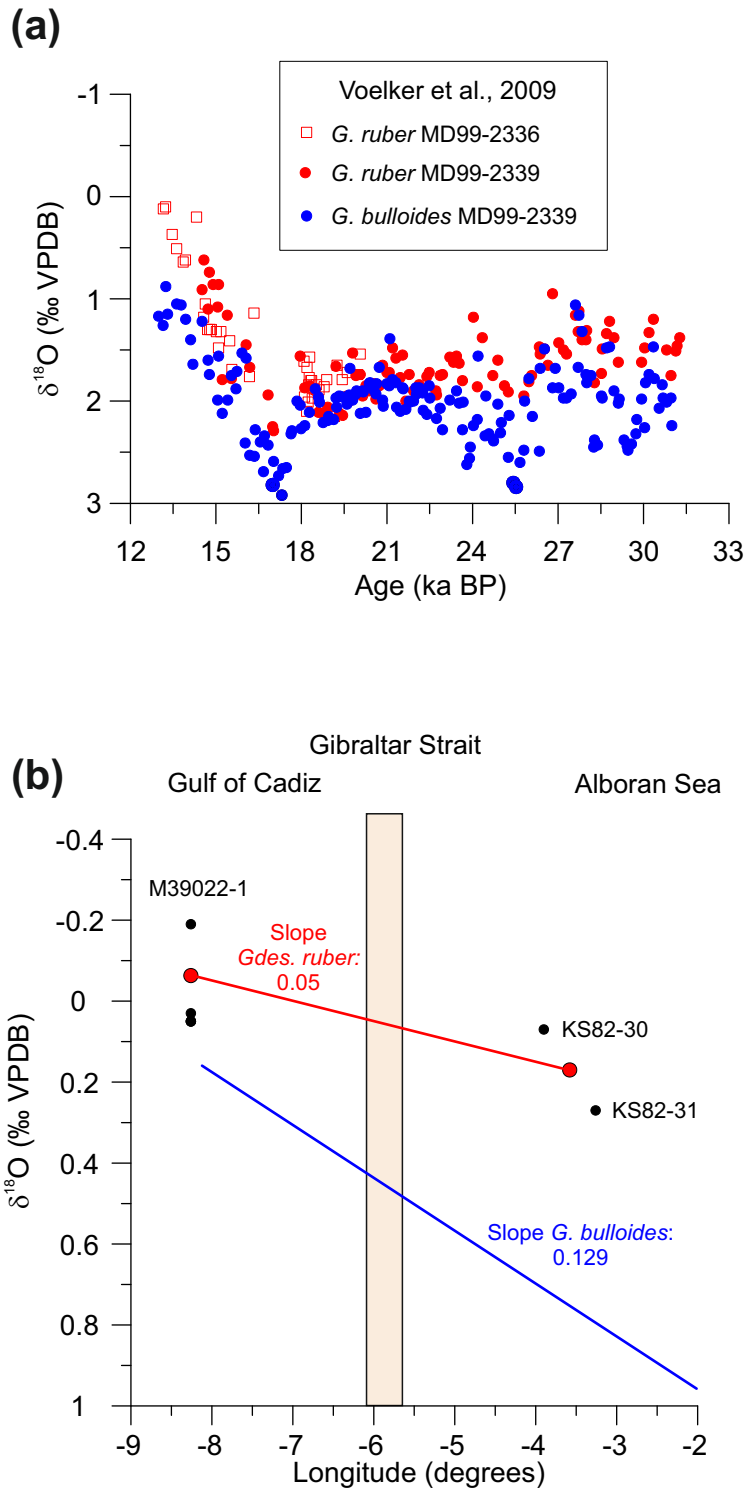
(a)
Voelker et al., 2009
G. ruber MD99-2336
G. ruber MD99-2339
G. bulloides MD99-2339
δ18O (‰ VPDB)
Age (ka BP)
(b)
Gibraltar Strait
Gulf of Cadiz
Alboran Sea
M39022-1
Slope
Gdes. ruber:
0.05
KS82-30
KS82-31
Slope G. bulloides:
0.129
δ18O (‰ VPDB)
Longitude (degrees)